Nephrol Dial Transplant (2018) 33: 224–230
doi: 10.1093/ndt/gfx243
Advance Access publication 15 September 2017

Metabolic imaging of fatty kidney in diabesity: validation and dietary intervention

Jacqueline T. Jonker[1,*], Paul de Heer[2,*], Marten A. Engelse[1], Evelien H. van Rossenberg[1], Celine Q.F. Klessens[3], Hans J. Baelde[3], Ingeborg M. Bajema[3], Sietse Jan Koopmans[4], Paulo G. Coelho[5], Trea C. M. Streefland[6], Andrew G. Webb[2], Ilona A. Dekkers[7], Ton J. Rabelink[7], Patrick C.N. Rensen[6,8], Hildo J. Lamb[7] and Aiko P.J. de Vries[1]

[1]Department of Nephrology, Leiden University Medical Center, Leiden, The Netherlands, [2]Department of Radiology, C.J. Gorter Center for High Field MR, Leiden University Medical Center, Leiden, The Netherlands, [3]Department of Pathology, Leiden University Medical Center, Leiden, The Netherlands, [4]Animal Science Group, Wageningen University and Research, Wageningen, The Netherlands, [5]Department of Biomaterials and Biomimetics, New York University College of Dentistry, New York University, New York, NY, USA, [6]Department of Endocrinology, Department of Medicine, Leiden University Medical Center, Leiden, The Netherlands, [7]Department of Radiology, Leiden University Medical Center, Leiden, The Netherlands and [8]Einthoven Laboratory for Experimental Vascular Medicine, Leiden University Medical Center, Leiden, The Netherlands

*These authors contributed equally to this work.
Correspondence and offprint requests to: Jacqueline T. Jonker; E-mail: j.t.jonker@lumc.nl

ORIGINAL ARTICLE

ABSTRACT

Background. Obesity and type 2 diabetes have not only been linked to fatty liver, but also to fatty kidney and chronic kidney disease. Since non-invasive tools are lacking to study fatty kidney in clinical studies, we explored agreement between proton magnetic resonance spectroscopy (^{1}H-MRS) and enzymatic assessment of renal triglyceride content (without and with dietary intervention). We further studied the correlation between fatty kidney and fatty liver.

Methods. Triglyceride content in the renal cortex was measured by ^{1}H-MRS on a 7-Tesla scanner in 27 pigs, among which 15 minipigs had been randomized to a 7-month control diet, cafeteria diet (CAF) or CAF with low-dose streptozocin (CAF-S) to induce insulin-independent diabetes. Renal biopsies were taken from corresponding MRS-voxel locations. Additionally, liver biopsies were taken and triglyceride content in all biopsies was measured by enzymatic assay.

Results. Renal triglyceride content measured by ^{1}H-MRS and enzymatic assay correlated positively ($r = 0.86$, $P < 0.0001$). Compared with control diet-fed minipigs, renal triglyceride content was higher in CAF-S-fed minipigs (137 ± 51 nmol/mg protein, mean ± standard error of the mean, $P < 0.05$), but not in CAF-fed minipigs (60 ± 10 nmol/mg protein) compared with controls (40 ± 6 nmol/mg protein). Triglyceride contents in liver and kidney biopsies were strongly correlated ($r = 0.97$, $P < 0.001$).

Conclusions. Non-invasive measurement of renal triglyceride content by ^{1}H-MRS closely predicts triglyceride content as measured enzymatically in biopsies, and fatty kidney appears to develop parallel to fatty liver. ^{1}H-MRS may be a valuable tool to explore the role of fatty kidney in obesity and type 2 diabetic nephropathy in humans *in vivo*.

Keywords: chronic kidney disease, fatty kidney, proton magnetic, resonance spectroscopy, renal triglyceride content, type 2 diabetes mellitus

INTRODUCTION

Over the past decades, the prevalence of obesity and type 2 diabetes has grown to epidemic proportions [1]. Obesity, in particular central obesity, is associated with metabolic dysfunction, which drives the development of insulin resistance leading to type 2 diabetes and ultimately end organ damage. The combination of obesity and type 2 diabetes, also referred to as diabesity, is often accompanied by other cardiovascular risk factors, including hypertension and dyslipidaemia. Common early markers of renal disease like glomerular hyperfiltration and increased urinary albumin are more prevalent in both obesity and type 2 diabetes [2]. Furthermore, renal pathology has shown considerable overlap between obesity and type 2 diabetes [3].

How (early) diabesity may lead to incipient chronic kidney disease remains to be understood, but ectopic lipid

accumulation in the kidney (fatty kidney) has gained appreciation as a novel potential pathway [2, 4–6]. Diabesity is associated with lipid accumulation in non-adipose tissue such as liver, skeletal muscle and heart, and this so-called ectopic fat may interfere with cellular function in the respective organ [7–10]. Notably, obesity and type 2 diabetes have been associated with renal lipid accumulation in both human and porcine kidneys with differences in anatomical distribution between glomeruli and tubuli, as well as cortex and medulla [11, 12]. Increased renal lipid content has also been linked to functional and structural renal hyperfiltration [12], obesity-related glomerulopathy [2] and type 2 diabetic nephropathy [13]. Various rodent models have shown that intervention in cellular lipid pathways attenuated obesity-related glomerulopathy or diet-induced chronic kidney disease [14]. To date, translation of such experimental evidence to the clinical arena has been hampered by lack of a non-invasive diagnostic tool to sequentially monitor renal lipid accumulation in obesity and type 2 diabetes mellitus.

Proton magnetic resonance spectroscopy (^{1}H-MRS) is a non-invasive and reproducible technique that has been used successfully to quantify lipid content in heart, liver and muscle [15–17]. Recently, feasibility and reproducibility of renal ^{1}H-MRS *in vivo* was shown [18]. However, few ^{1}H-MRS protocols have been validated against tissue biopsies.

Therefore, we explored the agreement of the non-invasive ^{1}H-MRS renal triglyceride measurement, using a 7-Tesla magnetic resonance (MR) scanner, against a biochemical assay (as gold standard) to determine lipid accumulation in of porcine kidneys. Secondly, we measured renal triglyceride content after a dietary intervention study in minipigs. We investigated the effects of a high-fat, high-cholesterol cafeteria diet without (CAF) and with low-dose streptozocin (STZ) (CAF-S) to induce non-insulin-dependent diabetes mellitus, compared with standard diet on renal and hepatic triglyceride content and distribution.

MATERIALS AND METHODS

Group A

Fourteen left-sided porcine kidneys were harvested from two Dutch pig slaughter lines. The kidneys were harvested within 30 min of termination to limit warm ischaemia time and were placed on ice. Kidneys were flushed with University of Wisconsin (UW) fluid and were scanned upon arrival. Tissue biopsies were taken from both the upper and lower pole of each kidney, immediately after scanning. The biopsy locations were visually matched to the areas where the ^{1}H-MRS measurements were performed. Biopsies were snap-frozen in liquid nitrogen and stored at −80°C.

Group B

A total of 15 Göttingen minipigs [19] were studied after they had been randomized to two different diets. The control group received a diet consisting primarily of barley, wheat and soya bean oil. The CAF group was fed a cafetaria diet [20], with a high content of lard, fructose, sucrose and added cholesterol. Five of the CAF-fed pigs were additionally treated with STZ after 5 months. The dose of STZ was individually adjusted to induce non-insulin-dependent diabetes to model type 2 diabetes. After 7 months of diet, the pigs were euthanized. Directly after termination, blood was drawn and a liver biopsy was taken. The whole study was executed at Ecole Veterinaire D'Alfort, France, and was approved by the local ethics committee for animal experiments. The same harvesting and analyses protocols performed for Group A were followed: left-sided kidneys were harvested with a maximum of 30 min warm ischaemia time, kidneys were flushed with UW fluid and transported to the hospital in the Netherlands on ice, for subsequent 7-Tesla MR scanning. After each MR scan, renal biopsies were taken from the corresponding MRS-voxel location of the upper and lower kidney poles. Biopsies were snap-frozen and stored at −80°C. For both Groups A and B, all kidneys had a maximum cold ischaemia time of 20 h before ^{1}H-MRS was performed.

Measurements

^{1}H-MRS. A 7-Tesla Philips Magnetic Resonance Imaging (MRI) scanner (Philips Healthcare, Best, The Netherlands) was used to measure renal triglyceride content by ^{1}H-MRS. A Nova quadrature transmit and 32-channel receive head coil (Nova Medical, Wilmington, MA, USA) was used for transmission and reception. A survey together with a Dixon water-fat scan was performed to position the MRS voxel ($10 \times 10 \times 10\,mm^3$) within the cortex of the kidney trying to avoid the medulla as much as possible [21]. On the Dixon scan fat image (Figure 1B) correct placement was confirmed, carefully avoiding extracellular (sinus or perirenal) lipids in the voxel. Secondly, measurements were performed in the upper and lower pole of each kidney. Stimulated echo acquisition mode (STEAM) spectra were acquired with an echo time of 8.2 ms without water suppression [repetition time (TR) 9 s, 3 averages] and with Multiply Optimized Insensitive Suppression Train (MOIST) water suppression (TR 3.5 s, 96 averages) [22, 23]. The MRS acquisition had a bandwidth of 3000 Hz and 4096 samples were acquired resulting in a spectral resolution of 0.73 Hz/sample. All spectra were fitted in the time-domain using the Java-based MR User Interface (jMRUI) [24]. The advanced method for accurate, robust and efficient spectral fitting (AMARES) algorithm was used to fit the resonances to a Gaussian line shape. Triglyceride content was calculated as a percentage of the (unsuppressed) water peak using the following equation:

$$TG = \frac{TG\,methyl(CH3) + TG\,methylene\,(CH2n)}{Water + TG\,methyl(CH3) + TG\,methylene(CH2n)} \times 100\% \quad (1)$$

where, TG = renal triglyceride content (%), TG methyl = area of the methyl resonance at 0.9 ppm (arbitrary unit), TG methylene = area of the methylene resonance at 1.3 ppm (arbitrary unit), Water = area of the water resonance (arbitrary unit).

Enzymatic measurement of lipids in renal and liver biopsy. The biopsies from the upper and lower pole of each kidney, as well as the liver biopsies, were snap-frozen in liquid nitrogen, homogenized and total lipids were extracted according to a modified protocol from Bligh and Dyer [25].

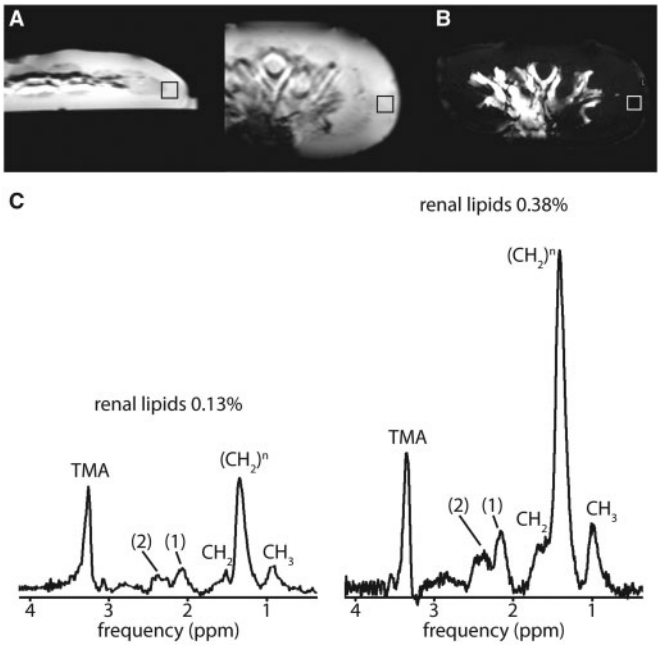

FIGURE 1: Placement of the voxel (black box) in the kidney cortex on a transverse and coronal survey **(A)** and Dixon fat image **(B)**. Below the surveys are two spectra (**C**) acquired from the kidney cortex of two different kidneys. Spectra have been selected to show an example of low and high renal triglyceride (TG) content and have been scaled to the water signal to be able to visually compare the two. For quantification of TG content the $(CH_2)^n$ (1.3 ppm) and the CH_3 (0.9 ppm) resonances are used. Other visible resonances in the spectra are CH_2CH_2COO marked with number 1 at 1.5 ppm, $CHCH_2 = CHCH_2$ marked with number 2 at 2 ppm and CH_2COO marked with number 3 at 2.2 ppm, and a trimethylamine (TMA) resonance at 3.2 ppm.

Total triglycerides were measured by an enzymatic kit (no. 11488872, Roche Diagnostics, Rotkreuz ZG, Switzerland). The triglyceride content per biopsy was divided by the protein content (nmol triglycerides/mg protein) to correct for the size of the biopsy.

Oil Red O staining. Frozen kidney sections (10 µm thickness) were cut on a Reichert cryostat microtome. Oil Red O (ORO) staining was performed by incubation of the slides with an ORO solution (2 mg/mL in 40% isopropanol). Sections were rinsed with ethanol, covered with Aqua-Mount mounting media and digitized with a Philips Ultra-Fast 1.6 RA Scanner (Philips, Best, The Netherlands). The ORO-positive surface area was measured using ImageJ (US National Institutes of Health, Bethesda, MD, USA) on five random selected areas of the renal cortex, and the percentage of the positive area was calculated.

Other laboratory measurements. Concentrations of plasma triglycerides and creatinine [both total coefficient of variation (CV): 1.0–1.2%, determined by vendor], urinary creatinine (total CV: 0.5–0.7%) and urinary protein (total CV: 0.2–0.6%) were measured on a Modular P800 analyser (Roche, Basel, Switzerland). Plasma fructosamine (total CV: 1.2–1.5%) was measured using a Cobas 6000 analyser (Roche).

Statistics

All statistical analyses were performed using SPSS version 22.0 (IBM SPSS Statistics for Windows, IBM Corp., Armonk, NY, USA). Plots were created using Graph Pad (Graph Pad Software, La Jolla, CA, USA). All but one analysis were performed with the average triglyceride content from the upper and lower pole of each kidney. Bland–Altman analysis was performed to evaluate the agreement between renal triglyceride content by ^{1}H-MRS and renal lipid content by enzymatic essay, after normalization of the data. In one case, the triglyceride content of a single pole was taken due to a corrupt MRS data file. Agreement between the triglyceride measurement techniques was evaluated by linear regression with a 95% prediction interval. Group differences between the three experimental groups were analysed using analysis of variance (ANOVA). Least significant difference (LSD) *post hoc* tests were used in case of a significant difference. Non-normally distributed data were log-transformed and checked for normality after transformation. Data are expressed as mean values ± standard error of the mean (SEM) and a probability value of ≤ 0.05 was considered statistically significant.

RESULTS

Validation of renal triglyceride quantification by ^{1}H-MRS

Renal triglyceride content was measured in 29 left-sided porcine kidneys by ^{1}H-MRS and by enzymatic assay. Two measurements had to be excluded from further analysis due to a failed measurement in the enzymatic assay and one due to a corrupt MRS data file, resulting in a total of 27 measurements ($n = 12$ from Group A, $n = 15$ from Group B).

In Group A (slaughter pigs), the mean renal triglyceride content was 0.23 ± 0.03% (mean ± SEM) as measured by ^{1}H-MRS and 111 ± 15 nmol/mg protein as measured by enzymatic assay. The mean renal triglyceride content in Group B (minipigs) was 0.15 ± 0.03% as measured by ^{1}H-MRS and 79 ± 20 nmol/mg protein as quantified by enzymatic assay.

Data from Groups A and B were pooled and triglyceride content measured by ^{1}H-MRS and enzymatic assay showed a positive correlation ($r = 0.86$, $P < 0.0001$, Figure 2). The regression equation was as follows: triglycerides measured by ^{1}H-MRS (%) = 0.03 + 0.0017 × triglycerides measured by enzymatic assay (nmol/mg). The triglyceride content for the pooled data ranged from 0.06% to 0.8% as measured by ^{1}H-MRS and from 30 to 331 nmol/mg protein as measured by enzymatic assay.

The Bland–Altman analysis using the normalized data showed good agreement with a bias of 0.00 (limits of agreement −0.8; 0.8) for ^{1}H-MRS and enzymatic essay measurements of renal lipid content over the metabolic spectrum (Figure 2B).

Effects of CAF and STZ

The minipigs were 2.7 ± 0.2 years of age at termination. The pigs in the control group were heavier at the start of the study (62.7 ± 3.3 kg, $P < 0.05$) than the pigs in the CAF group (51.4

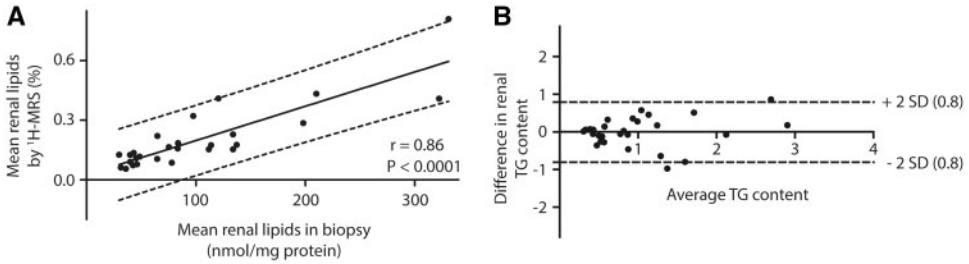

FIGURE 2: Correlation (left) and Bland–Altman difference–average plot (right) of renal triglyceride (TG) content measured by ^{1}H-MRS and enzymatic assay in biopsies, using pooled data from both Group A **(A)** (12 slaughter pigs) and Group B **(B)** (15 minipigs) showing a positive correlation ($R = 0.86$, $P < 0.0001$).

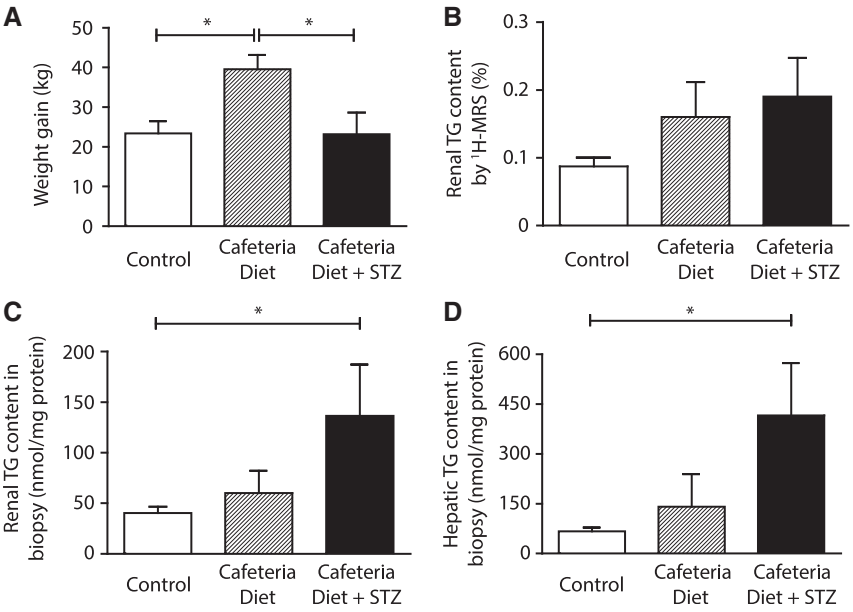

FIGURE 3: Weight gain **(A)**, renal triglyceride (TG) content measured by proton magnetic resonance spectroscopy (^{1}H-MRS, **B**), renal TG content from renal biopsy by enzymatic assay **(C)** and hepatic TG content from liver biopsy by enzymatic assay **(D)** after 7 months of control diet, CAF or CAF-S. Data are presented as mean ± SEM ($n = 15$ for renal triglycerides, $n = 14$ for hepatic triglycerides). *$P < 0.05$.

± 2.0 kg) and CAF-S group (49.7 ± 2.8 kg). The 7-month CAF induced a significantly larger weight gain (39.6 ± 3.6 kg) than the control diet (23.4 ± 3.1 kg, $P < 0.05$) and the CAF-S diet (23.2 ± 5.5 kg, $P < 0.05$, Figure 3). Serum fructosamine was higher in the CAF-S group (358 ± 31 µmol/L, $P < 0.05$), than in the CAF (264 ± 6 µmol/L) and control groups (259 ± 11 mol/L). Serum triglycerides, serum creatinine and urine protein did not significantly differ between the groups.

Renal triglyceride content was higher in the CAF-S group (137 ± 51 nmol/mg protein) compared with the control group (40 ± 6 nmol/mg protein, $P < 0.05$) (Figure 3). Renal triglyceride content in the CAF group (60 ± 10 nmol/mg protein) was not significantly different from the control group (Figure 3). Renal triglyceride content measured by proton MR spectroscopy showed a similar trend between the groups, however, this was not statistically significant.

Similarly, hepatic triglyceride content after the 7-month diet was higher in the CAF-S group (417 ± 157 nmol/mg protein) compared with the control group (67 ± 11 nmol/mg protein, $P < 0.05$). The CAF group (141 ± 49 nmol/mg protein) had a trend towards higher hepatic triglyceride content than the control group, but this was not significantly different (Figure 3). We observed a significant correlation between renal and hepatic triglyceride content measured by enzymatic assay ($n = 14$, $r = 0.97$, $P < 0.001$, Figure 4).

Lipid distribution

We also assessed lipid localization by ORO staining. The lipid content was very low in biopsies of the control diet group (percentage staining: 0.2 ± 0.0%), and markedly higher in those of the CAF group (3.7 ± 1.9%, $P < 0.05$ versus control diet) and CAF-S group (9.6 ± 6.3%, $P < 0.05$ versus control diet). There was pronounced lipid accumulation in the tubuli and to a lesser extent ORO staining was visible in the glomeruli (Figure 5).

DISCUSSION

The merit of clinical ^{1}H-MRS to investigate the role of ectopic lipid accumulation has been clearly established for other organs

such as liver, muscle and heart [17, 26, 27]. In fact, the development of ^{1}H-MRS of the heart has led to a better understanding of factors influencing myocardial triglyceride accumulation in relation to cardiac function in both health and diabesity [9, 17]. Our present study is one of the first to explore ^{1}H-MRS as a non-invasive tool to study fatty kidney in diabesity and to study agreement with tissue biopsies.

Thus far, only few studies have reported on ^{1}H-MRS of the kidney, most likely owing to the technical difficulties of developing and applying this technique reliably to the kidney for several reasons. Firstly, adjustment for respiratory motion and carefully avoiding contamination by perirenal and sinus fat is necessary to obtain reliable measurements from the kidney cortex only, and not surrounding structures. Secondly, kidney tissue is not homogenous with substantial anatomical and functional variation between cortex and medulla as well as glomeruli and tubuli. Lastly, due to the limited space in the kidney cortex, the volume of the measured voxel has to be small, resulting in a much lower signal-to-noise-ratio compared with e.g. heart and liver.

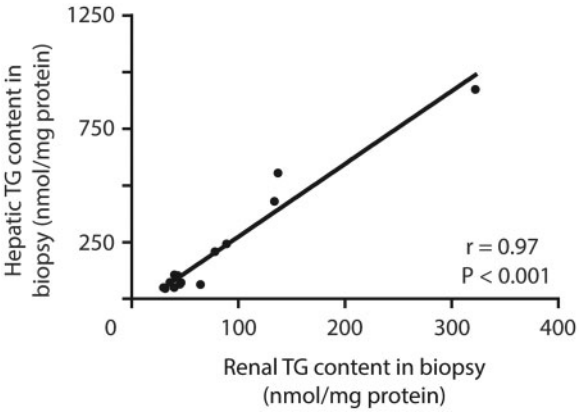

FIGURE 4: Correlation between renal and hepatic triglyceride (TG) content after 7 months of diet, measured by enzymatic assay in biopsies ($n = 14$).

This notwithstanding, we previously reported a feasibility and reproducibility study of renal ^{1}H-MRS in healthy (non-obese) volunteers *in vivo*, but variation was apparent even in this relative homogenous group of subjects [18]. Consequently, we aimed to improve our knowledge on triglyceride distribution across the metabolic spectrum of diabesity and across kidney anatomy with regard to voxel placement and data acquisition. Also, few spectroscopy protocols underwent validation and testing against invasive, gold standard assessment of triglycerides. Because of the impossibility of obtaining enough discarded kidneys from obese and type 2 diabetic post mortem kidney donors to perform a validation study (those kidneys are often not offered for transplantation), we turned to similar-sized porcine kidneys to test our clinical ^{1}H-MRS protocol. This study in porcine kidneys shows that ^{1}H-MRS closely predicts the triglyceride content as measured by enzymatic assay of kidney biopsies

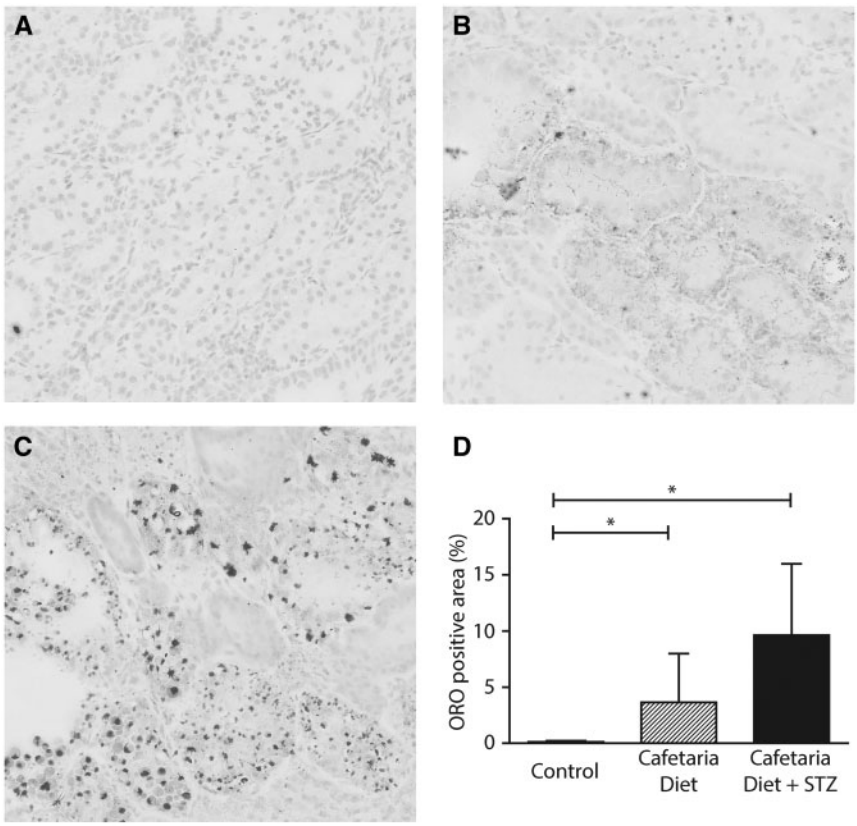

FIGURE 5: Three representative examples of ORO staining for lipids in kidney biopsies from minipigs on a 7 months control **(A)**, CAF **(B)** or CAF-S **(C)** diet. (**D**) Percentage of biopsy with ORO staining in the three diet groups (mean ± SEM, $n = 5$ per group). *P < 0.05 compared with the control diet.

(gold standard) and, therefore, it may also be a valuable tool to study fatty kidney in humans.

To evaluate the renal triglyceride content over the metabolic spectrum in conjunction with the hepatic triglyceride content, we used minipigs fed a high fat, high cholesterol diet to develop a metabolic syndrome phenotype including high amounts of visceral fat and insulin resistance [19]. Because those pigs have a large pancreatic beta cell capacity, it takes a very long time to develop type 2 diabetes. Therefore, the pigs were individually treated with a low dose of STZ to damage a part of the pancreatic beta cell capacity, to create non-insulin-dependent diabetes that reflects type 2 diabetes. Using this model, we showed that renal triglyceride content increased over the metabolic spectrum in conjunction with hepatic triglycerides.

We observed a trend to an increase in both renal and hepatic triglyceride content in the CAF-only group, however this was not significant. Previous studies have shown correlation between increased bodyweight and increased hepatic and renal triglyceride content in both animals and humans [11, 12, 28, 29]. As our study was exploratory and the animal groups small, the study may have been underpowered to detect a significant difference between the control and CAF group. One possible confounder in this study is the difference in baseline weight of the minipigs, as controls were significantly heavier than the pigs in the intervention groups.

Interestingly, pigs in the CAF-S group, albeit that they had a lower baseline weight and equal increase in body weight during the study, did have increased renal triglyceride content compared with the controls. In diabetes, the increase in inflammation or chronic kidney disease might lead to additional triglyceride redistribution into organs beyond mere obesity and thus accentuate the findings [2]. We found a strong positive correlation between renal and hepatic triglyceride content. A study in mice has shown that from a certain bodyweight, the expandability of white adipose tissue becomes limited and fat starts to rapidly accumulate ectopically within e.g. the liver [29]. It is likely that a similar mechanism may underlie renal triglyceride accumulation, which needs to be explored in future studies.

By using ORO staining, we observed similar trends, with increasing triglyceride content in the CAF group and even more in the CAF-S group. We found that renal triglyceride accumulation was most prominent in renal tubuli, albeit some triglyceride staining was also observed in the glomeruli. This is in accordance with a recent study of human nephrectomies, where triglyceride droplets were predominantly found in tubular cells and to a lesser extent in glomeruli [11]. Future studies should focus on even better understanding of how triglyceride accumulation may lead to chronic kidney disease in diabesity and whether this process can be reversed.

CONCLUSION

Non-invasive measurement of renal triglyceride content by ^{1}H-MRS closely predicts the triglyceride content as measured enzymatically in biopsies. Renal triglyceride content increases over the metabolic spectrum of diabesity and in the current study fatty kidney develops in parallel with fatty liver. ^{1}H-MRS seems suitable to explore the role of fatty kidney in obesity and type 2 diabetic nephropathy in humans *in vivo*.

ACKNOWLEDGEMENTS

Part of this work was presented at the ASN Kidney Week 2016 in Chicago. J.T.J. and P.H. are the guarantors of this work and, as such, had full access to all the data in the study and take responsibility for the integrity of the data and the accuracy of the data analysis.

FUNDING

This work was supported by the Dutch Kidney Foundation (innovation grant IP11.56) and the Netherlands Organisation for Scientific Research (NWO TOP grant 700.10.351). The *in vivo* part of the study was supported by ITI Research Grant number 926/2013.

CONFLICT OF INTEREST STATEMENT

None declared. All authors have fulfilled the criteria for authorship. A manuscript on the same or similar material has not already been published by us or has not been or will not be submitted to another journal by us or by colleagues at our institution before the work appears in *Nephrology Dialysis Transplantation*. Part of this work was presented orally at the ASN Kidney Week 2016 in Chicago.

REFERENCES

1. WHO. *Global Status Report On Noncommunicable Diseases* [article online]. http://apps.who.int/iris/bitstream/10665/148114/1/9789241564854_eng.pdf?ua=1 (3 August 2017, date last accessed)
2. de Vries AP, Ruggenenti P, Ruan XZ *et al.* Fatty kidney: emerging role of ectopic lipid in obesity-related renal disease. *Lancet Diabetes Endocrinol* 2014; 2: 417–426
3. Klessens CQ, Woutman TD, Veraar KA *et al.* An autopsy study suggests that diabetic nephropathy is underdiagnosed. *Kidney Int* 2016; 90: 149–156
4. Bobulescu IA. Renal lipid metabolism and lipotoxicity. *Curr Opin Nephrol Hypertens* 2010; 19: 393–402
5. D'Agati VD, Chagnac A, de Vries APJ *et al.* Obesity-related glomerulopathy: clinical and pathologic characteristics and pathogenesis. *Nat Rev Nephrol* 2016; 12: 453–471
6. Guebre-Egziabher F, Alix PM, Koppe L *et al.* Ectopic lipid accumulation: a potential cause for metabolic disturbances and a contributor to the alteration of kidney function. *Biochimie* 2013; 95: 1971–1979
7. Gastaldelli A, Cusi K, Pettiti M *et al.* Relationship between hepatic/visceral fat and hepatic insulin resistance in nondiabetic and type 2 diabetic subjects. *Gastroenterology* 2007; 133: 496–506
8. Perseghin G, Scifo P, De CF *et al.* Intramyocellular triglyceride content is a determinant of in vivo insulin resistance in humans: a 1H-13C nuclear magnetic resonance spectroscopy assessment in offspring of type 2 diabetic parents. *Diabetes* 1999; 48: 1600–1606
9. Rijzewijk LJ, van der Meer RW, Smit JW *et al.* Myocardial steatosis is an independent predictor of diastolic dysfunction in type 2 diabetes mellitus. *J Am Coll Cardiol* 2008; 52: 1793–1799
10. Snel M, Jonker JT, Schoones J *et al.* Ectopic fat and insulin resistance: pathophysiology and effect of diet and lifestyle interventions. *Int J Endocrinol* 2012; 2012: 983814

11. Bobulescu IA, Lotan Y, Zhang J *et al.* Triglycerides in the human kidney cortex: relationship with body size. *PLoS One* 2014; 9: e101285
12. Li Z, Woollard JR, Wang S *et al.* Increased glomerular filtration rate in early metabolic syndrome is associated with renal adiposity and microvascular proliferation. *Am J Physiol Renal Physiol* 2011; 301: F1078–F1087
13. Rutledge JC, Ng KF, Aung HH *et al.* Role of triglyceride-rich lipoproteins in diabetic nephropathy. *Nat Rev Nephrol* 2010; 6: 361–370
14. Wang XX, Jiang T, Shen Y *et al.* The farnesoid X receptor modulates renal lipid metabolism and diet-induced renal inflammation, fibrosis, and proteinuria. *Am J Physiol Renal Physiol* 2009; 297: F1587–F1596
15. de Heer P, Bizino MB, Lamb HJ *et al.* Parameter optimization for reproducible cardiac 1 H-MR spectroscopy at 3 Tesla. *J Magn Reson Imaging* 2016; 44: 1151–1158
16. Jonker JT, de Mol P, de Vries ST *et al.* Exercise and type 2 diabetes mellitus: changes in tissue-specific fat distribution and cardiac function. *Radiology* 2013; 269: 434–442
17. van der Meer RW, Doornbos J, Kozerke S *et al.* Metabolic imaging of myocardial triglyceride content: reproducibility of 1H MR spectroscopy with respiratory navigator gating in volunteers. *Radiology* 2007; 245: 251–257
18. Hammer S, de Vries AP, de Heer P *et al.* Metabolic imaging of human kidney triglyceride content: reproducibility of proton magnetic resonance spectroscopy. *PLoS One* 2013; 8: e62209
19. Koopmans SJ, Schuurman T. Considerations on pig models for appetite, metabolic syndrome and obese type 2 diabetes: from food intake to metabolic disease. *Eur J Pharmacol* 2015; 759: 231–239
20. Koopmans SJ, Dekker R, Ackermans MT *et al.* Dietary saturated fat/cholesterol, but not unsaturated fat or starch, induces C-reactive protein associated early atherosclerosis and ectopic fat deposition in diabetic pigs. *Cardiovasc Diabetol* 2011; 10: 64
21. Dixon WT. Simple proton spectroscopic imaging. *Radiology* 1984; 153: 189–194
22. Frahm J, Merboldt KD, Hanicke W. Localized proton spectroscopy using stimulated echoes. *J Magn Reson* 1987; 72: 502–508
23. Murdoch JB, Lampman DA. Beyond WET and DRY: optimized pulses for water suppression. *Proc Intl Soc Mag Reson Med* 1993: 1191
24. Naressi A, Couturier C, Devos JM *et al.* Java-based graphical user interface for the MRUI quantitation package. *MAGMA* 2001; 12: 141–152
25. Bligh EG, Dyer WJ. A rapid method of total lipid extraction and purification. *Can J Biochem Physiol* 1959; 37: 911–917
26. Boesch C, Machann J, Vermathen P *et al.* Role of proton MR for the study of muscle lipid metabolism. *NMR Biomed* 2006; 19: 968–988
27. Longo R, Pollesello P, Ricci C *et al.* Proton MR spectroscopy in quantitative in vivo determination of fat content in human liver steatosis. *J Magn Reson Imaging* 1995; 5: 281–285
28. van der Meer RW, Hammer S, Lamb HJ *et al.* Effects of short-term high-fat, high-energy diet on hepatic and myocardial triglyceride content in healthy men. *J Clin Endocrinol Metab* 2008; 93: 2702–2708
29. van Beek L, van Klinken JB, Pronk AC *et al.* The limited storage capacity of gonadal adipose tissue directs the development of metabolic disorders in male C57Bl/6J mice. *Diabetologia* 2015; 58: 1601–1609

Received: 27.2.2017; Editorial decision: 17.6.2017